MEKATRONIKA: JOURNAL OF INTELLIGENT MANUFACTURING AND MECHATRONICS
E-ISSN: 2637-0883
VOLUME 8, ISSUE 1, 2026, 28 - 42
DOI: https://doi.org/10.15282/mekatronika.v8i1.13472

RESEARCH ARTICLE

Emergent crowd behaviour analysis via interrelationship force modelling in pedestrian dynamics during evacuation processes using a bond graph

Ali Ahmed Allam, Azhar Mohd Ibrahim*, Suaib Al Mahmud, Hasmawati Antong, Khairul Affendy Md Nor

Advanced Multi-Agent System Lab, Department of Mechatronics Engineering, International Islamic University Malaysia, Malaysia

Abstract - Crowd dynamics simulation is important in transport station management, building evacuation, and massive public event safety management. Even though popular techniques like social force modelling and cellular automata with machine intelligence were previously employed to model evacuation, the limited representation of forces makes it difficult to comprehend individual behaviours affecting the overall crowd dynamics. The inability of the existing models to capture the crowd momentum inhibits the comprehension of crowd behaviour impact on crowd turbulence. To understand the emergent crowd behaviour by capturing the complex interplay of forces and energies associated with evacuation in a constrained scenario, this study introduces a bond graph model to represent interrelationship forces in pedestrian dynamics during evacuations. We propose transforming the bond graph model into a translation mechanical sub-model for performing a thorough analysis of momentum and effort variable rate changes. The simulations are conducted using 20SIM software, examining diverse scenarios with varying masses, locations, and closeness to exits to understand how people behave in different situations. Results obtained from the proposed model demonstrate that spatial constraints near walls affect momentum and the effort exerted toward surrounding pedestrians. Higher density of crowd leads to increased urgency to evacuate and results in longer time to reach the steady state. The proximity-based layered view shows pedestrians closest to the chosen pedestrian exerting the highest effort at a steady state. Additionally, when the chosen pedestrian is heavier than others, the effort exerted by him tends to be positive. Conversely, encountering heavier individuals may hinder movement, resulting in negative initial effort values. This study not only advances our understanding of pedestrian dynamics but also lays the groundwork for future research into the complex interrelationship forces at play in crowd movements and behaviours.

Article History
Received : 18 November 2025
Revised : 12 February 2026
Accepted : 6 June 2026
Published : 30 June 2026

Keywords
Bond graph modelling
Pedestrian dynamics
Social force model
Crowd evacuation

1. Introduction

Crowd simulation and modelling have attracted significant attention lately and have become central to multiple applications, including urban planning, event planning, transportation, architectural design, and evacuation modelling. This is particularly critical for the development of facilities involving emergent situations such as emergency evacuation modelling for disaster response [1], hospital evacuation [2], emergency evacuation from a stadium [3], and evacuation under terrorist attacks [4]. To execute effective evacuation modelling for such scenarios, understanding human and pedestrian dynamics is imperative. Studying pedestrian dynamics for emergency evacuation has been an ongoing research topic in traffic science and engineering. Since the early 1990s, this field has gained significant interest, demonstrating its critical importance [5]. Numerous approaches to simulate pedestrian dynamics and crowd behaviour have since emerged [6], [7]. However, there remain several avenues for further exploration within the research scope of crowd dynamics simulation. As noted by Yan et al. [8], crowds present one of the most challenging subjects for human behaviour modelling due to the multitude of influences on individual decision-making. Both social scientists and modellers have struggled to fully capture the diverse aspects of group behaviour. Pedestrian dynamics becomes more complex when a group of people is involved, known as a crowd. Collectively, the movement of such groups is referred to as crowd dynamics, which is bounded by multiple factors like congestion, urgency, etc., in emergent situations. Additionally, factors like distance from the exit, the number of evacuees near the exit, and the number of evacuees moving towards the exit were observed to have a huge influence on evacuees' behaviour during the evacuation process [9]. Considering crowd behaviour is of paramount importance when modelling crowd dynamics under emergencies. Understanding how each individual responds under such scenarios and how these responses are influenced by external factors is crucial for developing a successful model. Due to the high computational complexity of heterogeneous crowds, many challenges limit the realism of crowd simulation [10]. Previously, many research works were conducted to understand crowd behaviours and model evacuation scenarios, among which the Social Force Model (SFM), Cellular Automata (CA) and Rule-Based models are prevalent. The social force model (SFM) developed by Helbing et al. [11] is a commonly used microscopic model for predicting and analysing congestion, assessing building or urban layouts, and planning evacuation methods. In SFM, pedestrian movement is defined by the combination of different social forces affecting an individual. Helbing et al. [11] pioneered the study of crowd dynamics during escape panic by introducing the Social Force model, which integrates socio-psychological and physical forces to capture pedestrian behaviour during evacuations. Their simulations revealed how psychological and physical factors contribute to crowd behaviours, emphasising the importance of considering both aspects in evacuation planning. Yang et al. [12] investigated crowd behaviour in evacuation scenarios

***CORRESPONDING AUTHOR | Azhar Mohd Ibrahim** | ✉ azhar_ibrahim@iium.edu.my

using advanced computer simulations based on a modified Social Force model, highlighting the importance of individual decision-making processes in shaping overall crowd behaviour. Further research by Wei-Guo et al. [13] focused on subway station evacuations, modifying the social force model to account for different pedestrian types, including those carrying baggage and panic-stricken individuals. This modification provided a more accurate representation of evacuation behaviours in subway stations, highlighting the significance of diverse pedestrian classifications in evacuation simulations. These studies stress the importance of understanding individual behaviour in crowd simulation. However, despite the large number of studies carried out using SFM, the approach suffers from multiple issues and assumptions, such as homogeneous pedestrian characteristics, parameter sensitivity, scaling issues, etc. The traditional social force model (SFM) in crowd simulation has difficulty coping with the complexity of the crowd and is limited by a single set of physical formulas and parameters. Recent attempts to combine deep learning with these models focus more on simulating specific crowd states [14]. However, the inclusion of deep learning is highly time-consuming and requires manual hyperparameter tuning. These limitations make it difficult to model the crowd dynamics and lead to faulty solutions.

Cellular automata, on the other hand, is a branch of discrete dynamics that considers space as a regular grid and tracks changes in cells as time propagates in a discrete manner [15]. This particular model and its integration with soft computing techniques have been used in quite a few works for evacuation modelling as well as evacuee behaviour modelling [1], [4], [16], [17], [18]. However, although cellular automata and their variations are suitable for simple and fast implementation of crowd dynamics simulation, they include multiple shortcomings, such as neglecting additional free space and obstacles, the tendency of competition between pedestrians for open space, etc. [19]. Meanwhile, the rule-based models often require explicit expert knowledge of the systems and complex formulation of repetitive rules, which might halt the exploration of variation in real-world scenarios [20]. Such shortcomings in the available approaches, on the one hand, limit the capability to replicate the diversity in crowd dynamics; on the other hand, the limited representation of forces limits the capability to understand the complex behaviour of individuals in a heterogeneous crowd environment given the presence of different entities. Most existing crowd evacuation methods focus on internal factors and do not consider the influence of external environment factors [17]. Furthermore, although force-based models can capture individual motion, they cannot capture crowd momentum due to limited representation of interrelationships between forces and their directions. But capturing crowd momentum is extremely crucial, especially for modelling high crowd pressure and crowd turbulence in large gatherings, since crowds with higher momentum are more prone to disturbances that might eventually lead to more forceful interactions between people [21], [17]. Hence, understanding the crowd momentum can provide valuable insights into the complex interplay of forces in pedestrian dynamics during evacuation. To capture crowd momentum, it's extremely important to understand how external factors (obstacle proximity, individual weight, etc.) affect crowd behaviour while the crowd is lined up for evacuation.

Bond graphs can capture the momentum of components in a dynamic system by modelling the flow of forces and energies. By representing the flow of energies as a network of bonds and components as junctions, this approach provides a unified approach to system modelling, enabling researchers to analyse complex system behaviours and interactions, ultimately contributing to advancements in automation science and engineering. Bond graphs provide a domain-independent hierarchical framework for generating models based on physical and thermodynamic rules. Bond graphs, first proposed by Paynter [22], were designed primarily for technical purposes. Bond graph modelling emerges as a versatile technique for representing and analysing complex multidisciplinary systems, integrating different energy domains such as mechanical, electrical, and hydraulic components [23]. Oster et al. [14] expanded the use of bond graphs to the chemical domain, followed by Cellier [24]. Studies by Cheng et al. [25] and Benmoussa et al. [26] explore the application of bond graph modelling in understanding human-robot interaction dynamics and fault detection in mechatronic systems. This suggests that integrating bond graphs into evacuation modelling to understand pedestrian dynamics during evacuations could provide valuable insights into the interplay of forces and interactions within crowd dynamics. In this paper, we employed bond graph modelling with SFM to capture the complex interrelationships of forces and energy flow between pedestrians and obstacles in different scenarios and circumstances to understand the behaviour of the whole crowd under emergent situations. The goal is to understand how individuals would behave in an emergent situation given different obstacle positions and different characteristics of other individuals around them.

2. Materials and Methods

2.1 Social Force Modelling

The study is anchored in the foundational work of D. Helbing et al. [27] . This paper served as a basis for calculating essential parameters, including initial desired force ($F_{desired}$), interaction forces between pedestrians and walls (f_{iw}), and inter-pedestrian forces (fij). The relevant equations from the literature were adapted for application in current research[27]:

$$m_i \frac{dv_i}{dt} = \frac{m_i vo_i(t) eo_i(t) - v_i(t)}{\tau_i} + \sum\nolimits_{j \neq i} f_{ij} + \sum\nolimits_{w} f_{iw} \tag{1}$$

$$\tau_i = 0.5s \tag{2}$$

In Eq. (1), m_i represents the mass of pedestrian *I*, $vo_i(t) = 1\ m/s$ is the desired velocity of pedestrian *i* at time *t*. $eo_i(t)$ represents the desired direction of movement for pedestrian *i* at time *t*, whereas $v_i(t)$ and τ_i stand for the actual velocity of pedestrian *i* at time *t* and the relaxation time for pedestrian *I*, respectively. τ_i is technically a reasonable estimate for the relaxation acceleration time by Helbing et al. [11].

The interaction force between pedestrians is the repulsion force that prevents them from getting too close. When they do not touch, the interaction force between pedestrians *i* and *j* is given by Eq. (3) and Eq. (4):

$$f_{ij}^{rep} = A_i e^{(\frac{r_{ij}-d_{ij}}{B_i})} n_{ij} \quad (3)$$

$$r_{ij} = r_i + r_j \quad (4)$$

where $A_i = 2 * 10^3$ and $B_i = 0.08$ are constants for pedestrian *i*. r_{ij} and d_{ij} represent the sum of the pedestrians' radius and the actual distance between the pedestrians respectively. n_{ij} is the normalised direction from pedestrian i to j. On the other hand, the interaction force between pedestrians *i* and *j* when they do touch can be represented by:

$$f_{ij}^{touch} = A_i e^{\left(\frac{r_{ij}-d_{ij}}{B_i}\right)} + K_g\left(r_{ij} - d_{ij}\right)n_{ij} + \kappa_g\left(r_{ij} - d_{ij}\right)\Delta v_t^{ji} t_{ij} \quad (5)$$

$$\Delta v_t^{ji} = \left(v_j - v_i\right)t_{ij} \quad (6)$$

In Eq. (5) and Eq. (6), the body force constant which counteracts body compression is presented by $K_g 1.2 * 10^5$. $\kappa_g = 2.4 * 10^5$ is the sliding friction constant. t_{ij} is the tangential direction, and Δv_t^{ji} is the relative tangential velocity between pedestrians *i* and *j*. f_{ij}^{touch} accounts for both the repulsion and the friction when the pedestrians come into physical contact. In simulations, the correct force would be selected based on the distance d_{ij} compared to the sum of their radius r_{ij}. If $d_{ij} < r_{ij}$, then they are in contact, and the equation for them being in touch would be used. Otherwise, the equation without the pedestrians touching would be applied. Interaction of pedestrian *I* with walls W can be represented by Eq. (7):

$$f_{iw} = A_i e^{(\frac{r_i-d_{iw}}{B_i})} + K_g(r_i - d_{iw})n_{iw} - K_g(r_i - d_{iw})(v_i * t_{iw}) * t_{iw} \quad (7)$$

where d_{iw} is the distance of pedestrian *i* from the wall. n_{iw} is the normal direction from the pedestrian to the wall. t_{iw} is the tangential direction along the wall.

2.2 Bond Graph Modelling

To understand and model the intricacies of pedestrian dynamics during evacuation processes, this paper endeavours to represent the interrelationship forces as a translational mechanical sub-model system using the bond graph framework as shown in Figure 1. The aim of this approach was to capture the dynamic interactions among pedestrians, their environment, and the desired movement during evacuations. In this model, each pedestrian is conceptualised as a 1-junction where forces such as social interactions (F_{spring}), environmental influences like interaction with the wall ($F_{damping}$), and desired movement ($F_{desired}$) are introduced. This conversion enables us to move beyond classical mechanics and toward a more nuanced understanding of the forces shaping pedestrian behaviours during evacuations. Figure 2 shows the bond graph modelling of the translational mechanical system, which represents systems where translational motion is involved, such as the motion of masses along a straight path. The basic elements used in translational mechanical systems are inertia or mass (I: m), spring (C:1/k), damping (R: b), and effort sources (Se: F), which represent external forces. In Figure 1, M1 and M2 represent pedestrians, K/C represents mutual inter-pedestrian interaction, B/R represents environmental resistance, and F/Se represents the desired movement force.

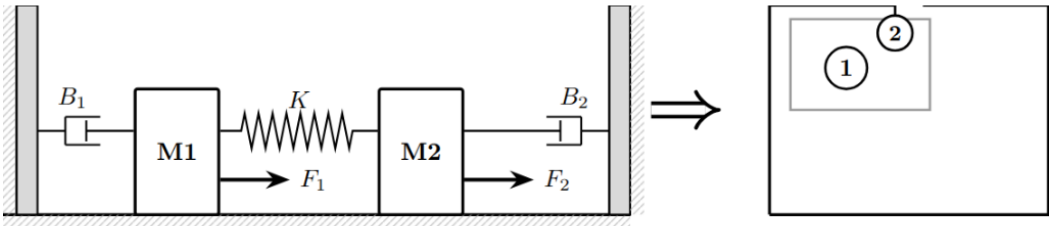

Figure 1. Equivalent representation of a two-mass translational mechanical system as two interacting pedestrians in an evacuation environment

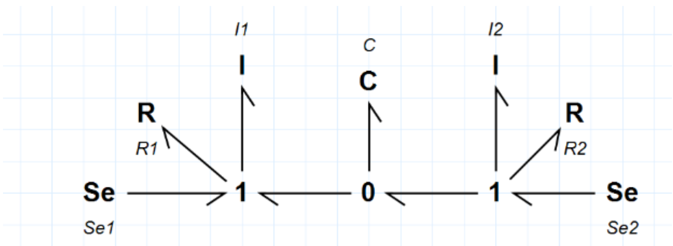

Figure 2. Bond graph modelling of two pedestrians

The output of the elements to the system are represented as follows:

$$Se_1: e_1 = m_1 \frac{V_1^0(t)e_1^0(t) - V_i(t)}{\tau_1} \tag{8}$$

$$I_1 = f_2 = \frac{P_1}{m_1} \tag{9}$$

$$R_1: e_3 = b_1 f_3 = b_1 f_2 = b_1 \frac{P_1}{m_1} \tag{10}$$

$$b_1 = \frac{f_{1,w}}{v_1} \tag{11}$$

$$b_1 = \frac{P_1}{m_1} \tag{12}$$

$$Se_2: e_8 = b_1 \frac{V_2^0(t)e_2^0(t) - V_2(t)}{\tau_2} \tag{13}$$

$$I_2: f_7 = \frac{P_2}{m_2} \tag{14}$$

$$R_2: e_9 = b_2 f_9 = b_2 f_7 = \ b_2 \frac{P_2}{m_2} \tag{15}$$

$$b_2 = \frac{f_{2,w}}{V_2} \tag{16}$$

$$C: e_5 = Kq \tag{17}$$

$$K = \frac{F_{1,2}}{X_{1,2}} \tag{18}$$

The inputs are received by the integral causality elements from the system and can be represented as below:

$$I_1: e_2 = \ e_1 - e_3 - e_4 \tag{20}$$

$$e_4 = e_5 \tag{21}$$

$$I_1: e_2 = m_1 \frac{V_1^0(t)e_1^0(t) - V_i(t)}{\tau_1} - b_1 \frac{P_1}{m_1} - Kq = \frac{dP_1}{dt} \tag{22}$$

$$C = f_5 = f_6 - f_4 \tag{23}$$

$$f_5 = \frac{P_2}{m_2} - \frac{P_1}{m_1} = \frac{dq}{dr} \tag{24}$$

$$I_1: e_7 = e_8 - e_6 - e_9 = \ m_2 \frac{V_2^0(t)e_2^0(t) - V_2(t)}{\tau_2} - -Kq - b_2 \frac{P_2}{m_2} = \frac{dP_2}{dt} \tag{25}$$

$$e_6 = e_5 \tag{26}$$

$$\begin{bmatrix} \frac{dP_1}{dt} \\ \frac{dP_2}{dt} \\ \frac{dq}{dt} \end{bmatrix} = \begin{bmatrix} \frac{-b_1}{m_1} & 0 & -K \\ 0 & \frac{-b_2}{m_2} & -K \\ \frac{-1}{m_1} & \frac{1}{m_2} & 0 \end{bmatrix} \begin{bmatrix} P_1 \\ P_2 \\ q \end{bmatrix} + \begin{bmatrix} m_2 \frac{V_2^0(t)e_2^0(t) - V_2(t)}{\tau_2} \\ m_1 \frac{V_1^0(t)e_1^0(t) - V_i(t)}{\tau_1} \\ 0 \end{bmatrix} \tag{27}$$

In bond graph analysis, interrelationship forces produce two key outputs: dp/dt and dq/dt . dp/dt typically represents the rate of change of momentum. In the context of pedestrian dynamics, this could be used to model the flow of pedestrians within the system. Positive values indicate acceleration, whereas negative values indicate deceleration. dq/dt signifies change in effort, reflecting forces among pedestrians and their environment. Positive dq/dt values indicate an increase in effort or force, while negative values indicate a decrease in effort.

In bond graph theory, power is defined as the product of effort and flow variables. In translational mechanical domains, effort corresponds to force while flow corresponds to velocity. Therefore, their product represents instantaneous mechanical power transfer within the system [6]. In the present pedestrian dynamics framework, effort represents the resultant social and environmental forces acting on each pedestrian, whereas flow corresponds to pedestrian velocity. Consequently, the effort-flow product quantifies the instantaneous mechanical work rate associated with pedestrian motion during evacuation. As established in Eq. (1), pedestrian motion follows Newtonian dynamics in the Social Force Model, where forces govern acceleration and momentum evolution. The mechanical power obtained from the bond graph formulation is directly related to the time rate of change of kinetic energy, providing a physically measurable quantity rather than a purely mathematical reformulation. Unlike conventional SFM implementations that focus primarily on force balance, the bond graph representation enables explicit tracking of energy storage (inertial elements), energy dissipation (resistive interactions), and power transmission between interacting pedestrians. This energy-based interpretation becomes particularly relevant under high-density evacuation conditions. Previous studies on crowd turbulence by Helbing et al. [21] demonstrated that hazardous situations arise from rapid momentum transfer and pressure amplification within dense crowds. The bond graph formulation allows these phenomena to be interpreted as localised power accumulation and dissipation processes, thereby providing additional physical insight into interaction dynamics beyond trajectory prediction alone. Accordingly, the proposed model represents not merely a mathematical transformation of the Social Force Model but an energetically consistent system representation capable of quantifying power exchange mechanisms within pedestrian crowds.

2.3 Considered Cases and Scenarios

To better understand how interrelationship forces act during evacuations by gaining insights into human reactions, group dynamics, and issues faced by larger groups, multiple scenarios were considered with varying numbers of pedestrians present. The spatial context specified was a square-shaped hall with an edge length of 4m. With vertices located at (0, 0), (0, 4), (4, 0), and (4, 4), the exit was placed in the middle of the front wall at the coordinate (2, 4). This physical configuration is critical for investigating situations with varying pedestrian numbers and comprehending the interaction of space restrictions, exit location, and interrelationship forces driving pedestrian behaviour during evacuations.

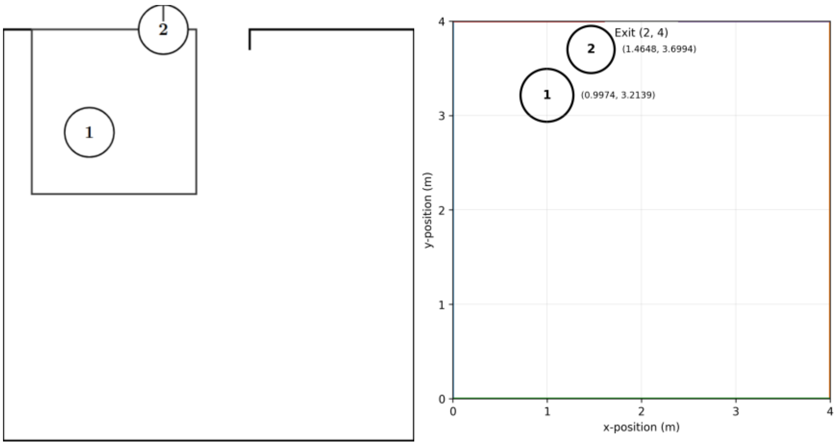

Figure 3. Positions of two pedestrians near the exit in the 4 m x 4 m hall

2.3.1 Case 1: Two Pedestrians at 3 Different Locations

Three scenarios have been considered under case 1, which includes 2 pedestrians for simulation. In these 3 scenarios, we examine the dynamics of 2 pedestrians with masses of 90 kg and 80 kg at 3 different locations in the hall. In the first scenario, the pedestrians with masses of 90 kg and 80 kg were positioned near the exit at (0.9974, 3.2139) and (1.4648, 3.6994), respectively, as shown in Figure 3. The interrelationship forces, including social interactions, environmental influences, and desired movement, were modelled using a Bond Graph as explained in Section 3. The calculations of the desired force ($F_{desired}$) are presented in Table 1, which plays the role of the SE component of the bond graph. The calculation of the inter-pedestrian forces F_{ij} to calculate the C component of the bond graph is shown in Table 2, and the calculation of the force exerted by the nearest wall F_{iw} , the R component of the bond graph, is presented in Table 3.

Table 1. Calculation of $F_{desired}$ of the two pedestrians who are nearest to the exit

Pedestrian i	Mass (kg)	$V_{desired}$ (m/s)	t	τ	Location	$F_{desired}$: $SE_{component}$ (N)
1	90	1	0.8	0.5	(1,3.21)	45
2	80	1	0.8	0.5	(1.46,3.7)	45

Table 2. Calculation of F_{ij} and C components of the two pedestrians nearest to the exit

i,j	d_{ij} (m)	r_{ij} (m)	F_{ij} (N)	$K = {F_{ij}}/{d_{ij}}$(N/m)	C=1/k (m/N)
1,2	0.67	0.53	330.91	491.03	0.002

Table 3. Calculation of F_{iw} and R components of the two pedestrians nearest to the exit

i	d_{iw}(m)	r_i(m)	V_i (m/s)	F_{iw} (N)	$R = F_{iw}/V_i$ (N.s/m)
1	0.7861	0.28	0.75	93953.89	125271.9
2	0.3006	0.25	0.56	7782.496	13835.55

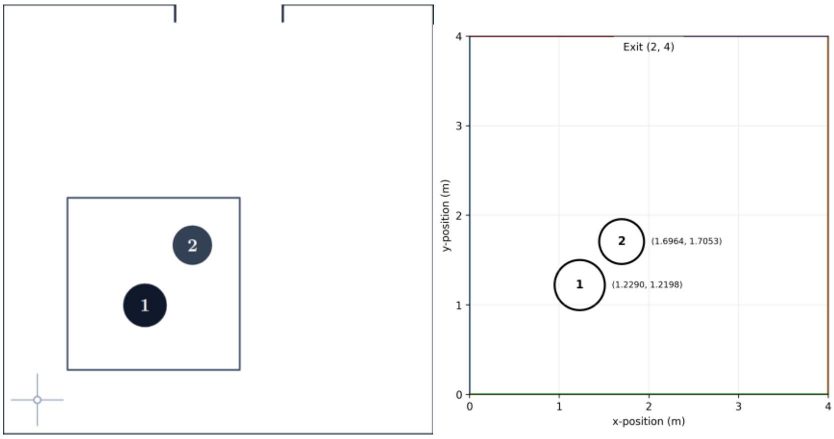

Figure 4. Positions of two pedestrians in the central region of the 4 m x 4 m hall

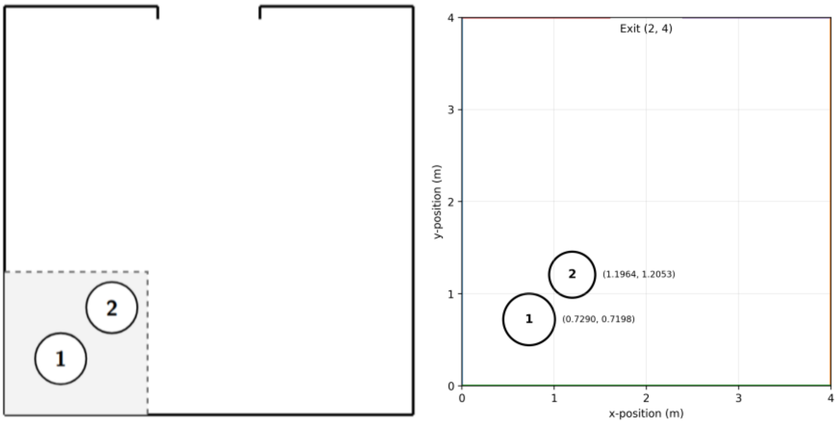

Figure 5. Positions of two pedestrians near the lower-left walls of the 4 m x 4 m hall

Subsequent scenarios explore similar setups, maintaining similar pedestrian masses while varying their positions by placing them at central space at coordinates (1.229, 1.2198) and (1.6964, 1.7053) for the second scenario (as shown in Figure 4) and near the walls at coordinates (0.729, 0.7198) and (1.1964, 1.2053) for the third scenario (as shown in Figure 5) within the evacuation space. For the second and third scenarios, as in the first, similar tables like Tables 1-3 are used to thoroughly examine the dynamics of pedestrian movement inside the constrained area. These tables provide computations relevant to the different situations, offering insights into the forces that influence pedestrian behaviour and evacuation dynamics. The bond graph shown in Figure 6 provides a framework for capturing the flow of forces and energies for the considered scenarios with 2 pedestrians.

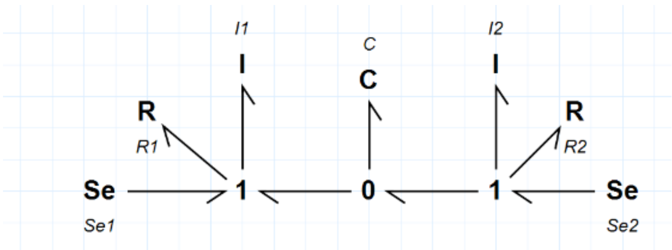

Figure 6. Bond graph of the 2 pedestrians nearest to the wall

2.2.2 Case 2: Pedestrians Positioned in a Central Space Within the Hall

This case implements the scenarios for more than 2 pedestrians in constrained places. The first 2 pedestrians were placed accordingly in a smaller square area in the hall with its vertices at (0.5, 0.5), (2, 0.5), (0.5, 2) and (2, 2). The smaller square area was designed to have an edge length of 1.5 m. The bond graph was then constructed for this scenario. Next, the number of pedestrians is increased to 3, 5 and 6 pedestrians. The additional pedestrians are placed adjacent to the previous pedestrians. It is noteworthy that while the number of pedestrians increases, the bond graph evolves accordingly, with the addition of junctions and components to accommodate the changing dynamics. The bond graph model, while remaining constant, adjusts to changing dynamics, representing the complexities of pedestrian interactions and their effect on crowd movement. Table 4 outlines the locations, mass, and radius of the 6 pedestrians, while the structure of the tables remains identical to those in case 1. Figure 7, Figure 8 and Figure 9 respectively represent the scenarios with 3, 5 and 6 pedestrians placed centrally into the hall, with the constructed bond graphs associated with them.

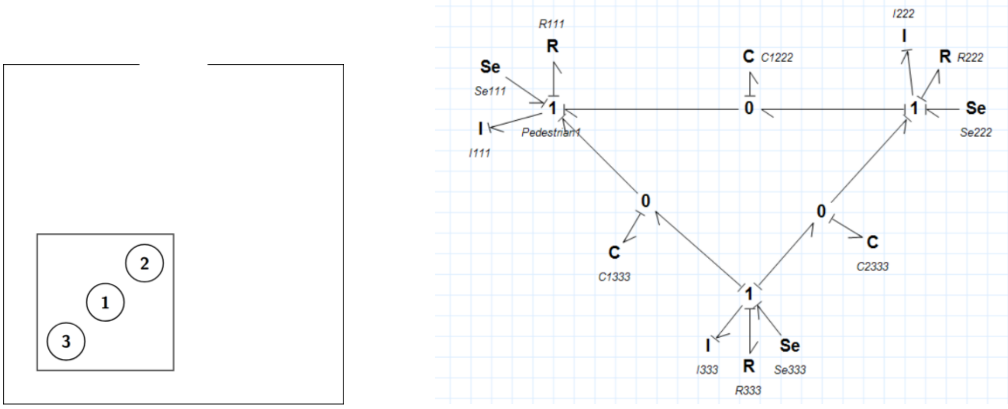

Figure 7. Centrally placed 3 pedestrians and bond graph

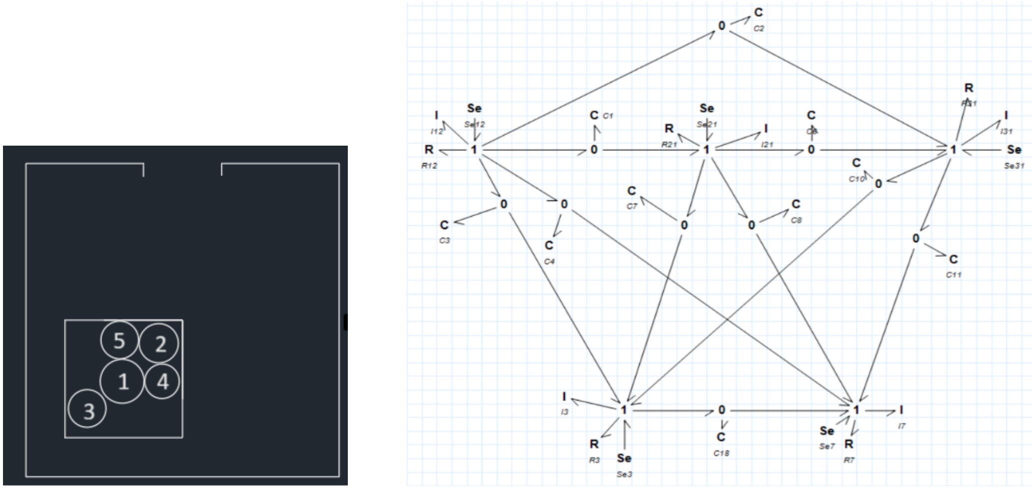

Figure 8. Centrally placed 5 pedestrians and bond graph

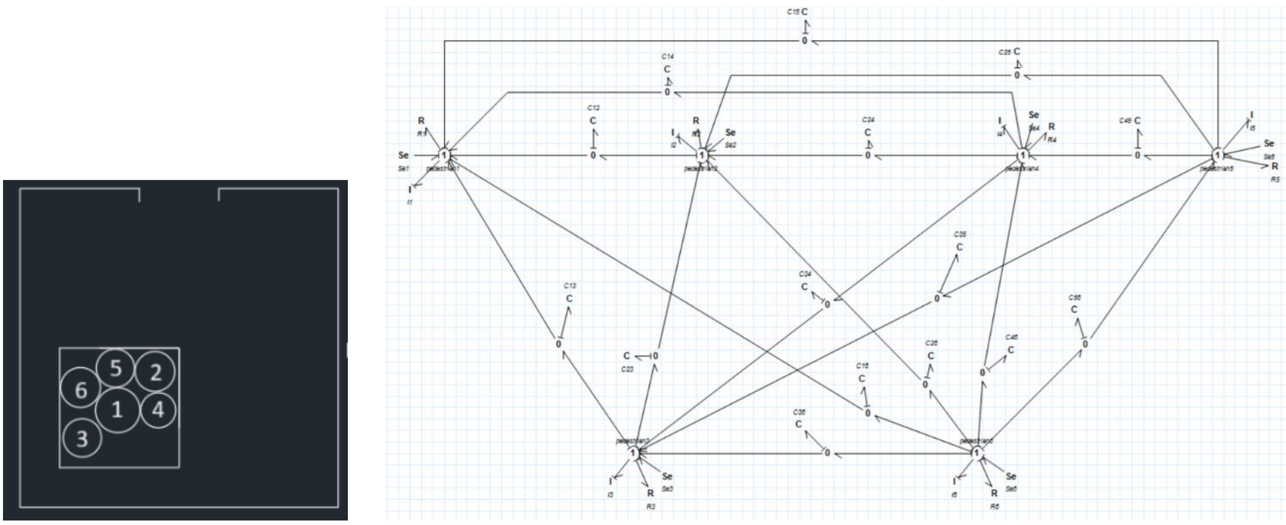

Figure 9. Centrally placed 6 pedestrians and associated bond graph

Table 4. Parameters of pedestrians positioned in a central space within the hall

I	Location	Mass (kg)	*r* (m)
1	(1.23,1.22)	90	0.28
2	(1.7,1.7)	80	0.25
3	(0.78,0.87)	70	0.24
4	(1.74,1.22)	50	0.22
5	(1.2,1.75)	70	0.24
6	(0.76,1.51)	80	0.25

2.2.3 Case 3: Pedestrians Positioned Around the Exit

This case involves placing pedestrians near the exit. 12 pedestrians were placed adjacent to each other near the exit as depicted in Figure 10. The higher number of pedestrians involved in the scenario increases the complexities in social interactions and navigation issues. It is important to note that while the structure of the tables remains identical to those in scenario 1, the input parameters such as pedestrian masses, distances to exits, nearest wall locations, and others change correspondingly. Table 5 outlines the locations, mass, and radius of the 12 pedestrians. Figure 10 represents the placement of 12 agents near the exit with the associated bond graph.

In the proposed study, the mass of pedestrians is selected as the primary demographic parameter because it directly appears in the governing motion equation of the Social Force Model, as defined in Eq. (1). Within this formulation, mass determines inertia and controls the rate of momentum evolution. In bond graph theory, effort corresponds to force and flow corresponds to velocity; therefore, inertia is represented through the I-element, which depends explicitly on mass [6]. Demographic attributes such as age, gender, and height do not directly modify the force balance but instead influence behavioural parameters including desired velocity v_0, relaxation time τ, and personal space radius, as demonstrated in empirical pedestrian investigations [9], [27]. These parameters affect decision-making and interaction distances rather than mechanical inertia. The objective of the present study is to establish an energy-consistent representation of pedestrian interactions using bond graph formalism. Introducing heterogeneous behavioural distributions simultaneously with the proposed modelling paradigm would obscure the interpretation of energy flow validation. Therefore, homogeneous behavioural parameters were intentionally adopted to isolate the mechanical contribution of interrelationship forces and verify the physical interpretability of power exchange. Future model extensions can incorporate demographic variability through stochastic distributions of desired velocity, relaxation time, and body radius implemented as variable source and resistive elements within the bond graph structure, allowing behavioural realism without altering the underlying energetic formulation.

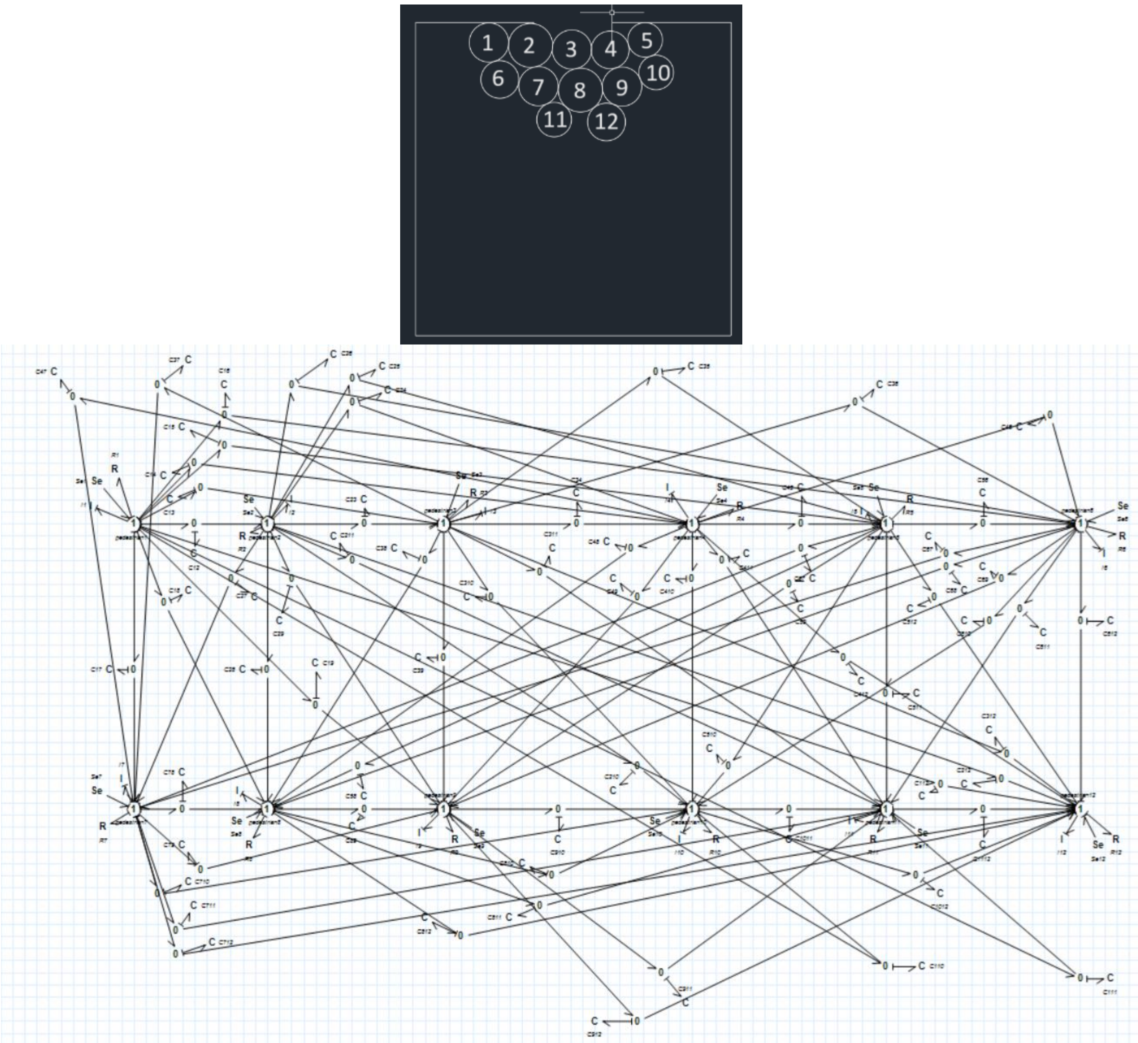

Figure 10. The 12 pedestrians' scenario

Table 5. Parameters of the 12 pedestrians' scenario

i	Location	Mass (kg)	r (m)
1	(0.929,3.7441)	80	0.25
2	(1.4564,3.7067)	90	0.28
3	(1.9806,3.6544)	80	0.25
4	(2.4657,3.6497	70	0.24
5	(2.9091,3.7775)	50	0.22
6	(1.0667,3.2721)	70	0.24
7	(1.5567,3.1864)	80	0.25
8	(2.0885,3.1368)	90	0.28
9	(2.6159,3.181)	80	0.25
10	(3.0493,3.3613)	50	0.22
11	(1.7551,2.7601)	50	0.22
12	(2.4189,2.7295)	70	0.24

3. Results and Discussion

The commercial software 20SIM was used to carry out the simulations of the developed models. Each scenario was simulated to reach the steady state to capture the behavioural decision-making scenario and its impact on the overall evacuation process. The outcomes from the simulation of each scenario are discussed below. The focus has been placed on the rate of change of momentum dp/dt and the change of effort variables of the occupants.

3.1 Case 1: Two Pedestrians at 3 Different Locations

As presented in section 4, this case involves placing 2 pedestrians having masses of 90 kg and 80 kg adjacent at different locations in the evacuation hall. Three scenarios, such as pedestrians located near the exit, at a central place in the hall and near the walls, have been examined. Figure 11 shows the momentum dynamics of Pedestrian 1 for three scenarios. It can be observed that, when the pedestrians were near the exit, Pedestrian 1's initial change in the rate of momentum was -93577.977, which decreased to a steady state of -2.65 very quickly within around 0.004 seconds, as represented by the pink curve. Similarly, when the pedestrians are placed centrally in the hall, the rate of momentum change for pedestrian 1 was calculated to be -121123.134 initially, which reached a steady state of -3.84 within less than 0.004 seconds, as represented by the red curve. However, when they were placed near the wall, the first pedestrian's initial change in momentum rate was recorded as -59645.097, which stabilised at -5.576 within around 0.005 seconds (represented by the cyan curve). The longer time taken to reach steady state when they are placed near the obstacle suggests that proximity to obstacles causes pedestrians to take more time to reach steady state during evacuation. The increase in initial rate of change in momentum suggests that, as pedestrians move away from walls and obstacles within the space, they experience a rise in momentum dynamics. This is because the decrease in initial momentum change rate when pedestrians are placed centrally in the hall indicates smoother and more rapid movement due to reduced constraints as pedestrians move away from obstacles (walls in this case). Hence, it can be said that when pedestrians are in proximity to obstacles, the haphazard movement contributes to a rise in the momentum dynamics and causes delay in reaching the steady state, which contributes to chaotic movement of the occupants, leading the whole system to a greater degree of crowd turbulence and making it more prone to disturbances [28]. This aggregation of chaotic movement, raising the degree of turbulence, could lead to hazardous situations by decreasing the efficiency of evacuation.

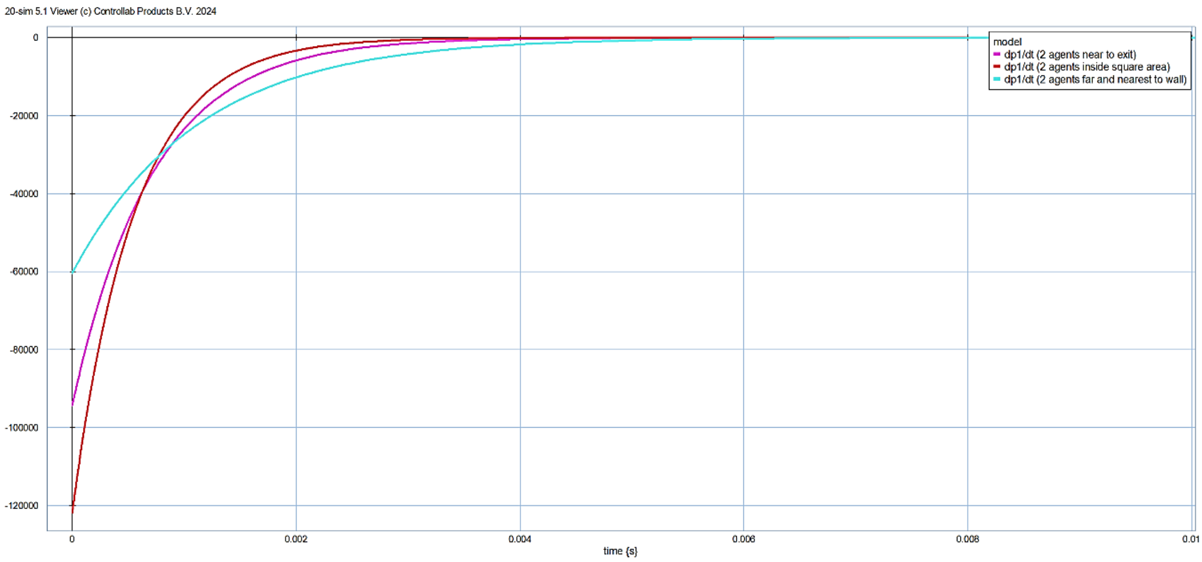

Figure 11. The rate of change in momentum of pedestrian1 for case 1 at 3 different scenarios

Figure 12 represents the change in effort variables for pedestrian 1 for all the considered scenarios in case 1. It can be observed that all the scenarios start with the same value of 0.1875 for the rate of effort change between Pedestrians 1 and 2. In Scenario 1 (marked by the green curve), a rapid decrease was seen in the rate of effort change, reaching a minimum of -0.362 at 0.002 seconds. This indicates low effort due to proximity to the exit. The value for change in effort then increases to a steady state of -0.0218 at 0.05 seconds, suggesting an increase of 93.98% as time passes by. Hence, it can be said that even though being close to the exit causes pedestrians to not exert much effort for evacuation, as time passes, they feel the urgency to evacuate and hence exert significantly more effort over time. As for the placement of the pedestrians in the central place of the hall, the rate of change in effort initially increased, reaching a maximum of 0.345 within 0.0002 seconds, before decreasing to a steady state of -0.0037 at 0.004 seconds. Similarly, in Scenario 3, when the pedestrians were placed near the walls (represented by the blue curve), the effort change rate initially rose to a maximum of 0.4 at 0.0004 seconds and then decreased to a steady state of -0.0058 within 0.009 seconds. It is apparent that Scenario 1 exhibits a more pronounced initial decrease in effort compared to Scenarios 2 and 3, likely due to its proximity to the exit. Moreover, in Scenario 2, where pedestrians are positioned in the middle of the hall, a quicker attainment of the steady state is expected compared to the other scenarios, likely due to lower urgency to evacuate and smoother movement, as indicated by the red curve. Hence, it can be said that crowd agglomeration is more likely to happen at the exit than in other places of the evacuation hall due to evacuees' heightened urgency for evacuation near the exit.

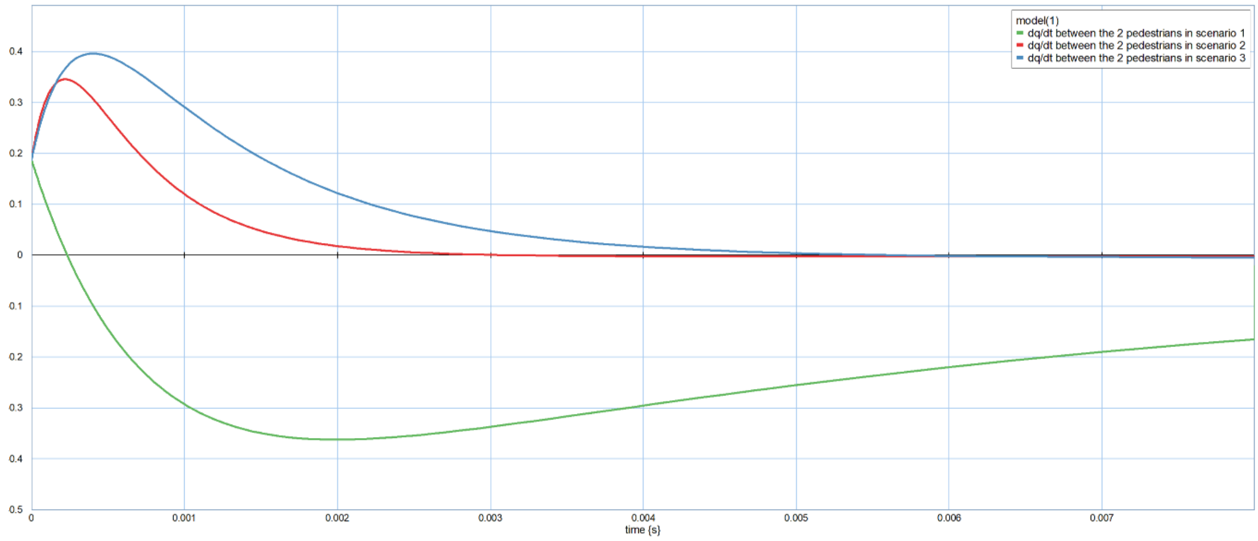

Figure 12. The effort variable rate of change of pedestrian1 across 2 pedestrians at 3 different locations scenarios

3.2 Case 2: Pedestrians Positioned in a Central Space Within the Hall

In this case, there are 4 scenarios where pedestrians are positioned within a smaller square area having an edge length of 1.5 m and its vertices at coordinates (0.5, 0.5), (2, 0.5), (0.5, 2), and (2, 2). Figure 13 illustrates the analysis of Pedestrian 1's dynamics across the considered evacuation scenarios for case 2. The emergence of distinct patterns reveals Pedestrian 1's adaptive responses to differing pedestrian densities. In the scenario with 2 pedestrians, Pedestrian 1 starts with a notably negative initial momentum of -121784.96 (red curve at 0s), gradually decreasing until reaching a near-zero steady state at 0.0089 seconds. Similarly, in scenarios with 3, 5, and 6 pedestrians, Pedestrian 1 exhibits a proportional increase in negative initial momentum values of -122916.05 (green curve), -126497.22 (purple curve), and -128066.43 (blue curve), respectively, indicating heightened urgency with increasing pedestrian density, which then gradually stabilises to near zero at steady state.

As more pedestrians surround pedestrian 1 during evacuation, the initial momentum of pedestrian 1 increases due to heightened urgency and obstacle perception. Increased pedestrian density raises awareness and urgency levels, driven by the need to navigate crowded areas and respond to social influences. Consequently, it takes more time for Pedestrian 1 to reach the steady state, reflecting the dynamic nature of pedestrian behaviour during evacuations. Additionally, in scenarios with varying pedestrian densities, such as those involving 2, 3, 5, or 6 pedestrians, the rate of change in Pedestrian 1's steady-state effort value decreases as the number of surrounding pedestrians increases. It's important to note that the negative sign does not imply a negative value in terms of the magnitude of momentum but rather the direction of change in momentum over time.

Figure 14 illustrates the change in rate of effort variable with distinct masses and positions within the defined area for case 2. Between Pedestrian 1 (90 kg) and Pedestrian 2 (80kg), the initial value started at 0.1875 (purple curve), increasing to a maximum of 0.34 at 0.0002 seconds, which subsequently decreased to a steady state of -0.031 at 0.003 seconds. Likewise, the interaction between Pedestrian 1 and Pedestrian 3 (70 kg) began at 0.25 (lime curve) and went directly to a steady state of -0.042 at 0.003 seconds. Unlike interactions with Pedestrians 2, 4, and 5, where peaks were observed in effort, interactions with Pedestrians 3 and 6 (80 kg) exhibit direct transitions to steady states without encountering an amplitude height. The initial values of effort rate change are inversely related to pedestrian mass, with heavier pedestrians yielding lower initial values. Furthermore, the increase in the value may be attributed to these pedestrians being positioned in front of Pedestrian 1 in the direction of the exit.

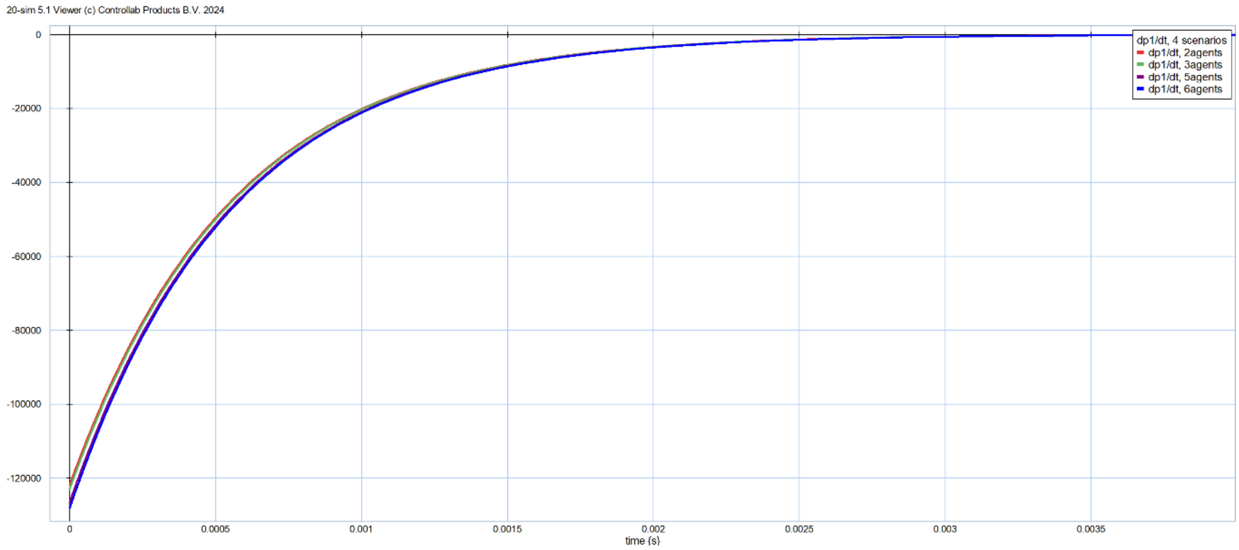

Figure 13. The rate of change of momentum of Pedestrian 1 across the 4 scenarios is placed centrally into the hall

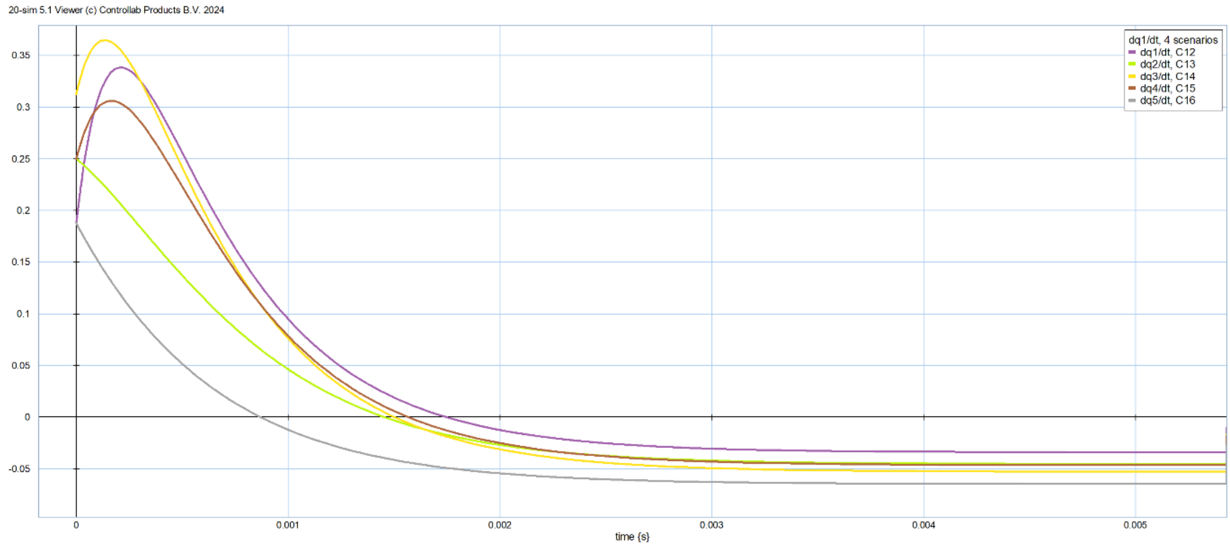

Figure 14. The rate of change in effort variable from the perspective of Pedestrian 1 within the scenario involving six pedestrians

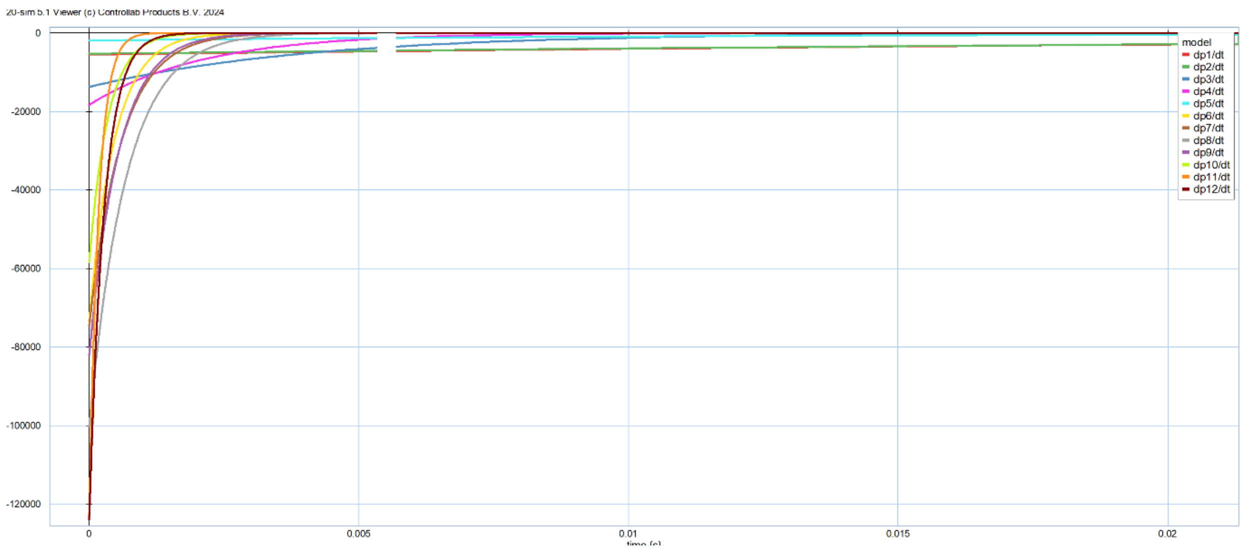

Figure 15. The momentum dynamics of the 12 pedestrians placed around the exit

3.3 Case 3: Twelve Pedestrians Around Exit

The momentum dynamics of twelve pedestrians in an evacuation scenario, as depicted in Figure 15, reveal diverse patterns. Pedestrian 1, represented by the red curve, started with an initial momentum rate change value of -5487.35, while pedestrian 2 (green curve) began at -5310.84. Pedestrian 3 (blue curve) showed an initial value of -13734.68, whereas that for pedestrian 4 (pink curve) was seen to be -18317.88. Meanwhile, pedestrian 5 (cyan curve), pedestrian 6 (yellow curve), pedestrian 7 (brown curve), pedestrian 8 (grey curve), pedestrian 9 (purple curve), pedestrian 10 (lime curve), pedestrian 11 (orange curve) and pedestrian 12 (burgundy curve) started with -1929.8, -73462.54, -74598.72, -100121.63, -82087.2, -58287.89, -123547.03, and -123872.6 respectively. The initial momentum dynamics vary based on proximity to obstacles like walls, influencing pedestrian momentum dynamics. Those closer to walls experience greater spatial constraints, resulting in lower initial momentum rate changes due to inhibited movement. This is attributed to environmental factors and perceptions of urgency and safety. Pedestrians farther from walls exhibit higher values for this particular variable. Additionally, pedestrians without others behind them, like pedestrians 10, 11, and 12, reached the steady state earlier compared to the ones in front, which indicates the tendency of allowance and patience among the evacuees who are behind in line when all of them are near the exit.

Figure 16 represents the change in the effort variable for the 12 pedestrians from the perspective of pedestrian 1. The pattern of values in the rate of change of the effort variable exhibits consistency among pedestrians with the same mass. For instance, interactions between pedestrian 1 and pedestrians 2 (red curve) and 8 (brown curve) began at -0.1875 at 0 seconds, indicating similar starting conditions. Similarly, interactions with pedestrians 3 (green), 7 (yellow), and 9 (grey) initiated at 0 seconds, while those with pedestrians 4 (blue), 6 (cyan), and 12 (orange) started at 0.0625 seconds. Meanwhile, interactions with pedestrians 5 (pink), 10 (purple), and 11 (lime) began at 0.125 at 0s.

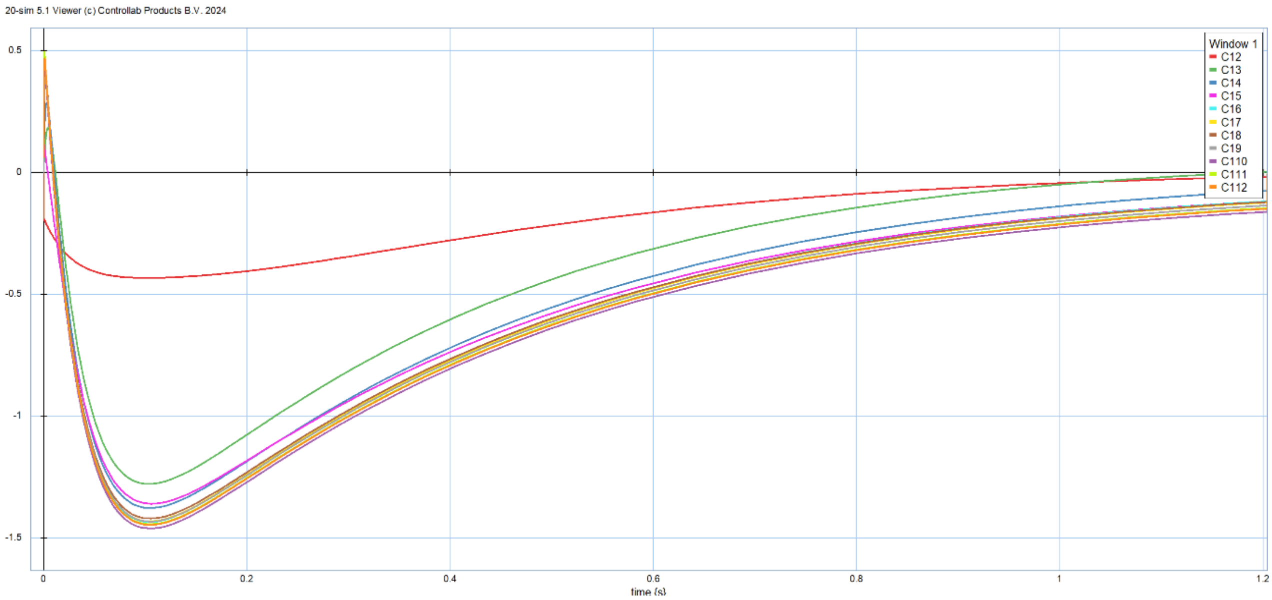

Figure 16. The rate of change of the effort variable of the 12-pedestrian scenario around the exit from the perspective of pedestrian 1

Initially, when pedestrian 1 encountered others, obstacles, or resistance, movement might have been hindered, causing a rapid decrease in charge. This decrease reflects the initial difficulty in response to the presence of other pedestrians. As time progressed, pedestrians adjusted their movements, leading to a gradual increase in effort towards the steady state. Analysis of the steady state reveals that the highest rate of effort change for pedestrian 1 was with pedestrian 6 (cyan curve). This value was followed closely for interactions with pedestrians 2, 3, 7, 4, 8, 11, 9, 5, 11, 12, and 10, respectively. The initial effort value exerted by pedestrian 1 toward others was consistent with that of pedestrians of the same mass. However, when the chosen pedestrian was heavier than others, the effort exerted was positive, suggesting an increase in effort as the mass of others decreases. Conversely, encountering heavier individuals might hinder movement, resulting in negative initial effort values. The steady-state comparison based on layers of evacuees illustrates a hierarchical influence on pedestrian 1. Layers, structured by proximity, show that pedestrians in Layer 1 who were closest to pedestrian 1, exhibited the highest values for rate of effort change. Within each layer, the first row consistently showed higher values, indicating a greater influence, which again bolsters the fact that the pedestrians close to the exit exhibit higher urgency for evacuation. This correlation highlights the effort required for pedestrian 1 to navigate past pedestrians in the same row toward the exit, providing insights into hierarchical influence during evacuations.

The simulations conducted in this study are based on a deterministic formulation where interactions between pedestrians are dictated solely by the force relationships described in Eq. (1). Identical initial and model parameters were intentionally maintained across scenarios to isolate the mechanical propagation of interrelationship forces within the bond graph framework. This controlled configuration enables direct interpretation of effort and flow power exchange without the influence of stochastic variability. Because the primary objective is validation of the bond graph representation rather than probabilistic evacuation prediction, single-run simulations are sufficient to demonstrate the model's mechanical consistency. Deterministic implementations of the Social Force Model have similarly been employed in foundational studies to analyse emergent crowd behaviours under controlled conditions [11]. Although pedestrian motion inherently exhibits variability arising from heterogeneous desired velocities, reaction times, and spatial distributions, the simulated pedestrian trajectories still allow qualitative interpretation of commonly discussed evacuation performance indicators. The results demonstrate variations in crowd congestion, interaction intensity, and spatial redistribution of pedestrians as movement progresses toward constrained regions such as exits and boundaries. These observable patterns correspond to performance descriptors frequently discussed in evacuation studies, including crowd accumulation near bottlenecks and density-dependent interaction behaviour [9], [11]. Future work will extend the current framework by introducing stochastic perturbations and multiple simulation realisations to perform Monte Carlo analyses, enabling statistical assessment while preserving the mechanical interpretation provided by the bond graph formulation.

3.4 Behavioural Validation

Three important behavioural validations emerge directly from the simulation results obtained using the proposed bond graph formulation. The initial observation concerns congestion formation near the exit area. As pedestrian density increases, individuals exhibit progressive velocity reduction accompanied by intensified interaction forces. This behaviour corresponds to the self-organised arching phenomenon widely reported in Social Force Model simulations introduced by Helbing et al. [11] and experimentally analysed in later crowd dynamics studies [10]. The fact that the bond-graph representation is similar proves that the basic mechanical behaviour of pedestrian evacuation is retained in the bond-graph representation. The second observation relates to momentum accumulation under high-density conditions. The results demonstrate increased interaction intensity and delayed stabilisation as pedestrian concentration grows. Such dynamics are consistent with crowd pressure build-up and turbulence mechanisms described by Helbing et al. [21], where force transmission between individuals generates collective motion instability during evacuation scenarios. Finally, the simulations reveal smooth trajectory adaptation and continuous interaction evolution rather than discrete positional transitions. This characteristic aligns with continuous-force pedestrian formulations and distinguishes the present approach from Cellular Automata models, which rely on spatial discretisation [16], [25]. The agreement in qualitative evacuation patterns confirms behavioural consistency between the proposed framework and established evacuation modelling paradigms. Together, these observations demonstrate that the bond graph formulation reproduces established evacuation behaviours while providing an energy-based interpretation of pedestrian interactions through effort-flow power exchange.

4. Conclusions

In this paper, the behaviour of evacuees was modelled using a combination of bond graph and social force modelling for multiple scenarios. It was seen that the proximity to obstacles, distance from the exit and the presence of other evacuees, along with their relative masses, significantly affect the behaviour of pedestrians in an evacuation scenario. It can be concluded that proximity to obstacles can induce heightened urgency among evacuees and can delay reaching steady state. Moreover, pedestrians near the exit can exhibit more urgency to evacuate than when they are away from the exit, which might result in higher crowd turbulence near the exit that might be prone to hazardous situations. Furthermore, evacuees seem to exert higher effort to evacuate when they are heavier than their adjacent pedestrians. Even though in a greater gathering, the presence of obstacles reduces momentum dynamics, resulting in decreased crowd turbulence, pedestrians near the exit feel more urgency to evacuate than those behind. Future work shall incorporate a comprehensive crowd evacuation simulation in a real-world setting using the bond graph model.

Acknowledgements

The authors acknowledge the support provided by the Sultan Ahmad Shah Medical Centre @IIUM (SASMEC @IIUM), International Islamic University Malaysia, in conducting this research.

Funding

This research was supported by grant SRG25-073-0073 awarded by the Sultan Ahmad Shah Medical Centre @IIUM (SASMEC @IIUM), International Islamic University Malaysia.

Declaration of Competing Interest

The authors declare that they have no conflicts of interest.

CRediT Authorship Contribution Statement

Ali Ahmed Allam: Conceptualization; Methodology; Data curation; Analysis; Writing - original draft;
Azhar Mohd Ibrahim: Supervision; Analysis; Writing- review & editing; Resources
Suaib Al Mahmud: Analysis and Discussion; Writing- review & editing
Hasmawati Antong: Supervision; Analysis and Discussion;
Khairul Affendy Md Nor: Supervision; Methodology; Analysis;

Availability of Data and Materials

The datasets generated and/or analysed during the current study are available from the corresponding author on reasonable request.

Ethics Declarations
This study did not involve human participants or animals. Ethical approval was therefore not required.

Generative Artificial Intelligence Declarations
Generative artificial intelligence tools were used solely to improve readability and language quality. All scientific content, analyses, interpretations, and conclusions were reviewed and approved by the authors, who take full responsibility for the manuscript.

References

[1] Liu J, Chen Y, Chen Y. Emergency and disaster management-crowd evacuation research. Journal of Industrial Information Integration. 2021;21:100191. https://doi.org/10.1016/j.jii.2020.100191
[2] Abir IM, Ibrahim AM, Toha SF, Shafie AA. A review on the hospital evacuation simulation models. International Journal of Disaster Risk Reduction. 2022;77:103083. https://doi.org/10.1016/j.ijdrr.2022.103083
[3] Helbing D, Buzna L, Johansson A, Werner T. Self-organized pedestrian crowd dynamics: Experiments, simulations, and design solutions. Transportation Science. 2005;39(1):1-24. Available: https://api.semanticscholar.org/CorpusID:14262793
[4] Liu Q. A social force model for the crowd evacuation in a terrorist attack. Physica A: Statistical Mechanics and its Applications. 2018;502:315-330. https://doi.org/10.1016/j.physa.2018.02.136
[5] Schadschneider A, Chowdhury D, Nishinari K. Pedestrian Dynamics. Elsevier; 2011. https://doi.org/10.1016/B978-0-444-52853-7.00011-7
[6] Rasouli A. Pedestrian simulation: A review. 2021. Available: http://arxiv.org/abs/2102.03289
[7] Khan S, Deng Z. Agent-based crowd simulation: An in-depth survey of determining factors for heterogeneous behavior. The Visual Computer. 2024. https://doi.org/10.1007/s00371-024-03503-2
[8] Yan D, Ding G, Huang K, Bai C, He L, Zhang L. Enhanced crowd dynamics simulation with deep learning and improved social force model. Electronics. 2024;13(5). https://doi.org/10.3390/electronics13050934
[9] Haghani M, Sarvi M. Stated and revealed exit choices of pedestrian crowd evacuees. Transportation Research Part B: Methodological. 2017;95:238-259. https://doi.org/10.1016/j.trb.2016.10.019
[10] Wang GN, Chen T, Chen JW, Deng K, Wang RD. Simulation of crowd dynamics in pedestrian evacuation concerning panic contagion: A cellular automaton approach. Chinese Physics B. 2022;31(6). https://doi.org/10.1088/1674-1056/ac4a67
[11] Helbing D, Farkas I, Vicsek T. Simulating dynamical features of escape panic. Nature. 2000;407(6803):487-490. https://doi.org/10.1038/35035023
[12] Yang X, Dong H, Wang Q, Chen Y, Hu X. Guided crowd dynamics via modified social force model. Physica A: Statistical Mechanics and its Applications. 2014;411:63-73. https://doi.org/10.1016/j.physa.2014.05.068
[13] Wei-Guo S, Yan-Fei Y, Bing-Hong W, Wei-Cheng F. Evacuation behaviors at exit in CA model with force essentials: A comparison with social force model. Physica A. 2006;371(2):658-666. https://doi.org/10.1016/j.physa.2006.03.027
[14] Oster GF, Perelson AS, Katchalsky A. Network thermodynamics: Dynamic modelling of biophysical systems. Quarterly Reviews of Biophysics. 1973;6(1):1-134. https://doi.org/10.1017/S0033583500000081
[15] Farrell R, Moallemi M, Wang S, Xiang W, Wainer G. Modeling and simulation of crowd using cellular discrete event systems theory. In: Proceedings of the 2013 ACM SIGSIM Principles of Advanced Discrete Simulation; 2013. p. 159-168. https://doi.org/10.1145/2486092.2486114
[16] Li D, Han B. Behavioral effect on pedestrian evacuation simulation using cellular automata. Safety Science. 2015;80:41-55. https://doi.org/10.1016/j.ssci.2015.07.003
[17] Liang H, Yang L, Du J, Shu CW, Wong SC. Modelling crowd pressure and turbulence through a mixed-type continuum approach. Transportation B. 2024. https://doi.org/10.1080/21680566.2024.2328774
[18] Liu T, Yang X, Wang Q, Zhou M, Xia S. A fuzzy-theory-based cellular automata model for pedestrian evacuation from a multiple-exit room. IEEE Access. 2020;8:106334-106345. https://doi.org/10.1109/ACCESS.2020.3000606
[19] Yu T, Yang HD. Simulation of running crowd dynamics: Potential-based cellular automata model. IEEE Access. 2023;11:138602-138613. https://doi.org/10.1109/ACCESS.2023.3336914
[20] Fu L, Song W, Lo S. A fuzzy-theory-based method for studying the effect of information transmission on nonlinear crowd dispersion dynamics. Communications in Nonlinear Science and Numerical Simulation. 2017;42:682-698. https://doi.org/10.1016/j.cnsns.2016.06.025
[21] Helbing D, Johansson A, Al-Abideen HZ. Crowd turbulence: The physics of crowd disasters. Physical Review E. 2007. Available: http://arxiv.org/abs/0708.3339
[22] Paynter HM. Analysis and Design of Engineering Systems. Cambridge, MA: MIT Press; 1961. Available: https://api.semanticscholar.org/CorpusID:106867876
[23] Uddin SU, Rideout G. Dynamic modelling and analysis of solar powered reverse osmosis desalination system for Pakistan using the bond graph model. In: IEEE International IoT, Electronics and Mechatronics Conference; 2022. https://doi.org/10.1109/IEMTRONICS55184.2022.9795841
[24] Cellier FE. Modeling chemical reaction kinetics. In: Continuous System Modeling. New York: Springer; 1991. p. 347-416. https://doi.org/10.1007/978-1-4757-3922-0_9

[25] Cheng PJ, Ting HY, Huang HP. Importing the human factor into safe human-robot interaction function using the bond graph method. Robotica. 2021;39(5):772-786. https://doi.org/10.1017/S0263574720000715
[26] Benmoussa S, Bouamama BO, Merzouki R. Bond graph approach for plant fault detection and isolation: Application to intelligent autonomous vehicle. IEEE Transactions on Automation Science and Engineering. 2014;11(2):585-593. https://doi.org/10.1109/TASE.2013.2288697
[27] Helbing D, Molnar P. Social force model for pedestrian dynamics. Physical Review E. 1995;51(5):4282-4286. https://doi.org/10.1103/PhysRevE.51.4282
[28] Chen C, Sun H, Lei P, Zhao D, Shi C. An extended model for crowd evacuation considering pedestrian panic in artificial attack. Physica A: Statistical Mechanics and its Applications. 2021;571:125833. https://doi.org/10.1016/j.physa.2021.125833